Virologica Sinica 41 (2026) 58–69

Contents lists available at ScienceDirect

Virologica Sinica

journal homepage: www.keaipublishing.com/en/journals/virologica-sinica
www.virosin.org

Research Article

Integrated multiplex PCR and metatranscriptomics reveal upper-lower airway microbial landscapes in pediatric respiratory infections

Peilan Wei [a,b,c,d,1], Lu Zhang [e,1], Qingtao Hu [b,c,1], Airu Zhu [b,c,1], Zhen Zhuang [b,c,1], Zhaoyong Zhang [b,c], Shengnan Zhang [b], Jiantao Chen [b], Xinyi Xiong [f], Bin Qu [f], Yuanyuan Zhang [b], Lei Chen [b], Zhiwei Xu [b], Zhao Chen [b], Qier Zhong [b,g], Xindan Xing [b], Xinxin Li [b], Jingjing Gao [b], Yifang He [b], Guifei Xie [b], Juan Shang [g], Xiaoke Guo [g], Jiaxin Jiang [b], Yongxia Shi [d], Jingxian Zhao [b,c,d,*], Yanqun Wang [b,c,g,h,*], Jincun Zhao [b,c,d,f,*], Yingkang Jin [a,*]

[a] Pediatric Pulmonary Department, Guangzhou Women and Children's Medical Center, Guangzhou Medical University, Guangzhou 510623, China
[b] State Key Laboratory of Respiratory Disease, National Clinical Research Center for Respiratory Disease, National Center for Respiratory Medicine, Joint International Research Laboratory of Respiratory Health, Guangdong Basic Research Center of Excellence for Respiratory Medicine, Guangzhou Institute of Respiratory Health, The First Affiliated Hospital of Guangzhou Medical University, Guangzhou 510182, China
[c] China-Portugal Artificial Intelligence and Public Health Technologies Joint Laboratory, Guangdong-Hong Kong-Macao Joint Laboratory of Respiratory Infectious Diseases, Guangdong Provincial Key Laboratory of Respiratory Disease Research, Guangzhou Medical University, China
[d] Guangzhou National Laboratory, Bio-Island, Guangzhou 510000, China
[e] Health and Quarantine Laboratory, State Key Laboratory of Respiratory Disease of Guangzhou Customs District Technology Center, Guangzhou 510623, China
[f] Shanghai Institute for Advanced Immunochemical Studies, School of Life Science and Technology, ShanghaiTech University, Shanghai 201210, China
[g] GMU-GIBH Joint School of Life Sciences, Guangzhou Medical University, Guangzhou 511436, China
[h] School of Basic Medical Sciences, Guangzhou Medical University, Guangzhou 511436, China

ARTICLE INFO

Keywords:
Pediatric ARTIs
Microbial landscapes
Bronchoalveolar lavage
Metatranscriptomics
Antimicrobial resistance

ABSTRACT

Despite widespread use of multiple PCR, a substantial proportion of pediatric acute respiratory tract infections (ARTIs) lack identifiable pathogens and are classified as unknown etiology. The microbial characteristics and clinical relevance of these cases remain unclear. In this study, we compared the airway microbiomes of PCR-positive and PCR-negative ARTIs and examined their relationships with sampling site and disease severity. A total of 514 hospitalized children with ARTIs were enrolled. Nasopharyngeal swabs (NS) and bronchoalveolar lavage fluid (BALF) samples were tested using a 22-target multiplex PCR panel and subsequently stratified by pathogen status for pooled metatranscriptomic sequencing to profile active microbial communities, viral genotypes, and antibiotic resistance genes. PCR identified common respiratory pathogens in 77.0% of NS and 54.1% of BALF samples. Metatranscriptomic analysis showed that PCR-negative pools displayed markedly lower viral activity and comparatively higher bacterial transcript abundance, with notable enrichment of *Pseudomonas*. Microbial signatures differed between upper and lower airway samples and across clinical severity, with severe cases demonstrating increased bacterial burden and *Pseudomonas* enrichment, whereas mild infections exhibited relatively stronger viral signals. Under current thresholds, antibiotic resistance genes were detected in patient pools but not in healthy controls. Overall, PCR-negative pediatric ARTIs exhibited distinct, bacteria-enriched microbial profiles. Integrating metatranscriptomics with PCR enhances pathogen characterization and reveals site- and severity-related microbial patterns that may support diagnostic evaluation and clinical management.

* Corresponding authors.
E-mail addresses: yingkangjin@163.com (Y. Jin), zhaojincun@gird.cn (J. Zhao), wangyanqun@gird.cn (Y. Wang), zhaojingxian@gird.cn (J. Zhao).
[1] Peilan Wei, Lu Zhang, Qingtao Hu, Airu Zhu, and Zhen Zhuang contributed equally to this work.

https://doi.org/10.1016/j.virs.2026.02.001
Received 26 August 2025; Accepted 28 January 2026
Available online 5 February 2026

INTRODUCTION

Acute respiratory tract infections (ARTIs) remain a major cause of childhood morbidity and mortality worldwide. According to the World Health Organization, ARTIs account for approximately 1.3 million deaths annually in children under five, with pneumonia responsible for the most fatalities (Um et al., 2023). Despite advances in diagnostic technologies, the precise etiological identification of respiratory pathogens remains a clinical challenge. This is largely due to the broad spectrum of potential viral and bacterial agents, their frequent co-infections, and limitations of current routine molecular assays, which typically target only a restricted panel of common pathogens (Yang and Rothman, 2004; Candel et al., 2024). Consequently, a substantial proportion of pediatric ARTIs remains etiologically unexplained, and patients are often managed empirically with supportive care or broad-spectrum antibiotics, highlighting the urgent need for more comprehensive pathogen surveillance strategies.

The respiratory tract can be anatomically divided into upper and lower compartments, each with distinct tissue structures and microbial communities. Infections often originate in the upper airway and may progress to the lower tract, leading to more severe conditions such as pneumonia (Man et al., 2017). Characterizing microbial differences between upper and lower respiratory tract infections (URTI vs. LRTI) provides critical insights for early diagnosis and clinical management (Kelly et al., 2025; Zelasko et al., 2025). In addition to anatomical variation, disease severity also shapes microbial composition. Comparative analyses between mild and severe cases can reveal specific taxa associated with clinical progression (Galeeva et al., 2024; Wang D. et al., 2025). Moreover, profiling antimicrobial resistance genes (ARGs) helps identify emerging resistance patterns and guide empirical antibiotic use (Waskito et al., 2022; Bai et al., 2025). Together, comprehensive evaluation of microbial signatures across anatomical sites, disease severity, and resistance landscapes is essential for improving diagnostic accuracy and targeted treatment strategies in pediatric ARTIs.

To address these critical clinical and scientific gaps, we conducted a large-scale, systematic study of hospitalized children with ARTIs across different age groups. We comprehensively analyzed both upper respiratory (nasopharyngeal swab, NS) and lower respiratory (bronchoalveolar lavage fluid, BALF) samples using a dual approach: conventional multiplex PCR to detect 22 common respiratory pathogens and metatranscriptomic next-generation sequencing (mNGS) to investigate pathogen-negative cases. This study aimed to delineate the viral and bacterial spectrum in both known and undiagnosed ARTI cases, compare the microbial landscapes of upper versus lower respiratory tract infections, and explore associations between microbial features and clinical disease severity. By integrating molecular diagnostics and high-resolution sequencing, our findings provide novel insights into the respiratory virome and microbiome in pediatric ARTIs and offer a valuable framework for future pathogen surveillance and precision diagnostics.

RESULTS

Demographic and clinical characteristics of participants

A total of 514 children (≤ 14 years) diagnosed with ARTI were enrolled at Guangzhou Women and Children's Medical Center between December 2020 and July 2021. Nasopharyngeal swabs (NS, n = 505) and bronchoalveolar lavage fluid (BALF, n = 85) samples were collected from ARTI patients. Healthy children (n = 24) without respiratory symptoms were recruited as controls, and nasopharyngeal swabs were obtained from these individuals (Fig. 1). The male-to-female ratio among patients was 1.73:1 (326:188). Patients were stratified into four age groups: 0–1 year (n = 130), 1–2 years (n = 170), 3–5 years (n = 163), and 6–14 years (n = 51). The median age was 2.1 years (interquartile range, 0.92–4.00), with an overall age range of 1 month–14 years (Table 1). Based on clinical diagnoses (Harris et al., 2011), 59 patients had severe pneumonia, 375 had pneumonia, and 80 had other respiratory infections. Detailed demographic and clinical data are summarized in Table 2. Disease severity was assessed for each ARTI patient using a previously described scoring system (Bradley et al., 2011).

Similar pathogen profiles identified in upper and lower respiratory tracts by multiplex PCR

A total of 505 NS and 85 BALF samples from ARTI patients were analyzed using a 22-target multiplex PCR assay. Respiratory pathogens were detected in 77.0% (389/505) of NS samples and 54.1% (62/85) of BALF samples (Fig. 2). In NS specimens, the most common pathogens were human metapneumovirus (HMPV) (27.13%), human rhinovirus/

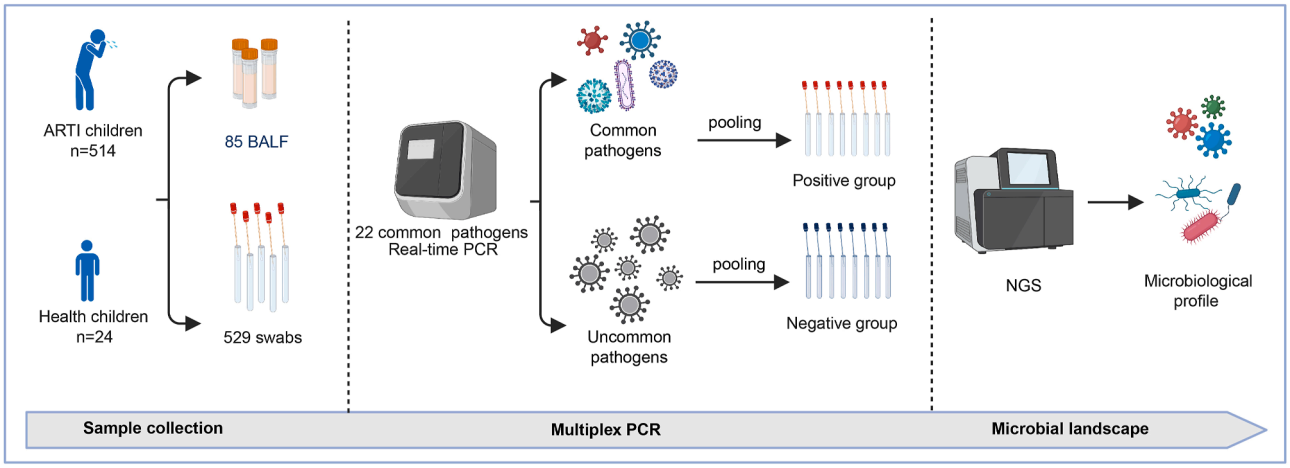

Fig. 1. Study design and workflow. Respiratory samples from pediatric patients with acute respiratory tract infection (ARTI) were analyzed in a two-step process. In the first step, 22 common respiratory pathogens were detected using real-time multiplex PCR, targeting human adenovirus (HAdV), human bocavirus (HBoV), common human coronaviruses (HCoV-229E/OC43/NL63/HKU1), human metapneumovirus (HMPV), influenza A (FluA), influenza B (FluB), pandemic H1N1 (H1N1pdm09), human parainfluenza virus types 1–4 (HPIV1/2/3/4), human rhinovirus/enterovirus (HRV/EV), respiratory syncytial virus A and B (RSV-A, RSV-B), *Bordetella pertussis* (BP), *Chlamydia pneumoniae* (CP), *Legionella pneumophila* (LP), and *Mycoplasma pneumoniae* (MP). In the second step, samples from pathogen-positive and pathogen-negative groups were pooled and subjected to metatranscriptomic next-generation sequencing (NGS) for comprehensive microbial profiling. Abbreviations: ARTI, acute respiratory tract infection; BALF, bronchoalveolar lavage fluid; NGS, next-generation sequencing.

Table 1
Baseline demographic characteristics of pediatric patients with acute respiratory tract infection.

Characteristics	Acute respiratory tract infection individuals	Healthy individuals
No. of individuals	514	24
Gender, n (%)		
Male	326 (64.4)	15 (62.5)
Female	188 (36.6)	9 (37.5)
Age, n (%)		
<1 year	130 (25.3)	8 (30.0)
1–2 years	170 (33.1)	6 (25.0)
3–5 years	163 (31.7)	2 (15.0)
6–14 years	51 (9.9)	8 (30.0)
Sample type		
Nasopharyngeal swabs	505	24
BALF	85	0
Clinical diagnosis, n (%)		
Severe pneumonia	59 (11.5)	0
Pneumonia	375 (73.0)	0
Other diagnosis[a]	80 (15.5)	0

[a] Represents bronchitis, trachitis, respiratory tract infection and so on.

Table 2
Information of nasopharyngeal swabs and bronchoalveolar lavage fluid samples in this study.

Characteristics	Nasopharyngeal swabs	Bronchoalveolar lavage fluid samples
No. of samples	505	85
Gender, n (%)		
Male	319 (63.2)	15 (62.5)
Female	186 (36.8)	23 (37.5)
Age, n (%)		
<1 year	126 (25.0)	16 (18.8)
1–2 years	168 (33.3)	21 (24.7)
3–5 years	162 (32.1)	27 (31.8)
6–14 years	49 (9.7)	21 (24.7)
Clinical diagnosis, n (%)		
Severe pneumonia	57 (11.3)	26 (30.6)
Pneumonia	370 (73.3)	50 (58.8)
Other diagnosis[a]	78 (15.4)	9 (10.6)

[a] Represents bronchitis, trachitis, respiratory tract infection and so on.

enterovirus (HRV/EV) (26.53%), and human bocavirus (HBoV) (9.5%), with a co-infection rate of 28.53% (111/389) (Fig. 3A). BALF samples showed a similar pattern, with HRV/EV (32.94%), human adenovirus (HAdV) (15.29%), HMPV (11.76 %), and HBoV (11.76%) being most frequently detected (Fig. 3B). Co-infections were present in 25.81% (16/62) of pathogen-positive BALF samples. Most co-infections involved two pathogens, while cases involving three pathogens were rare (Fig. 2A).

Pathogen distribution varied by age. HMPV, HRV, and respiratory syncytial virus (RSV) were predominant in infants under 1 year, while HRV, HMPV, HBoV, RSV, and human parainfluenza virus 3 (HPIV3) were common in the 1–2-year group. In children aged 3–5 year, HMPV, HRV, HBoV, HAdV, and human parainfluenza virus 4 (HPIV4) dominated, and in those over 6 years, HMPV, HRV, and HAdV were most prevalent. RSV, HBoV, and HPIV showed significant age-related differences (Fig. 2B). HMPV detection peaked in children aged 3–5 years. A male predominance in infection was observed across all 22 pathogens (Fig. 2C). HRV/EV was the most common virus in severe pneumonia cases (Fig. 2D). Notably, only one NS sample (0.2%) tested positive for influenza.

Phylogenetic analysis reveals predominant genotypes of circulating respiratory viruses

To further characterize the genetic diversity of the most prevalent respiratory viruses detected in ARTI patients, we conducted gene-specific amplification (Supplementary Table S1) and phylogenetic analyses on the top five viral pathogens. The analyses revealed distinct patterns of genotype circulation during the study period. HMPV strains were predominantly clustered within subtype B, indicating a dominant circulation of the B lineage (Supplementary Fig. S1). HRV exhibited the highest diversity, with genotype A being the most prevalent, followed by genotype C (Supplementary Fig. S2). HBoV strains were uniformly classified as HBoV1 (Supplementary Fig. S3), consistent with previous reports highlighting its predominance in respiratory infections (Wang Y. et al., 2016). RSV strains were largely of the BA.9 genotype, a well-documented subgroup within RSV-B known for its global dissemination in recent years (Hou et al., 2024) (Supplementary Fig. S4). HAdV displayed the greatest genotypic heterogeneity, with multiple co-circulating genotypes identified, including HAdV-C1, C2, C5, and C6 (Supplementary Fig. S5). These results underscore the ongoing genetic evolution and co-circulation of diverse viral genotypes among pediatric ARTI patients, which may have implications for diagnostic sensitivity, clinical severity, and vaccine design.

Distinct viral landscapes in pathogen-positive and pathogen-negative groups identified by metatranscriptomic sequencing

Following multiplex PCR screening, 116 of 505 NS samples and 23 of 85 BALF samples tested negative for the 22 targeted respiratory pathogens. Based on PCR results, clinical samples were stratified into pathogen-positive (PG) and pathogen-negative (NG) groups. Within each group, eight individual samples were randomly pooled and subjected to mNGS (Fig. 1). High-quality reads were aligned to in-house IDseq microbial reference databases, enabling comprehensive detection of bacterial, viral, fungal, parasitic, and unclassified microbial sequences in both NS and BALF specimens (Fig. 4A). Distinct microbial signatures were observed between PG and NG groups. In NS samples, the mean proportions of mapped reads corresponding to bacteria, viruses, and other microorganisms were 70.90%, 11.65%, and 17.43% in the PG group, compared with 81.45%, 0.65%, and 17.90% in the NG group, respectively (Fig. 4A). Similarly, in BALF samples, the corresponding values were 81.45%, 5.45%, and 13.10% in PG, and 84.09%, 0.03%, and 15.87% in NG (Fig. 4B). Virus-associated reads were significantly more abundant in PG samples, particularly in the upper respiratory tract, whereas bacterial reads were enriched in NG samples ($P < 0.05$, Fig. 4A and C). These findings suggest that viral infections predominate in pathogen-positive cases, while undetected bacterial pathogens may underlie a substantial proportion of pathogen-negative cases.

We next characterized the virome composition within PG and NG groups. The most frequently detected viral families included *Picornaviridae*, *Pneumoviridae*, and *Paramyxoviridae*, consistent with the major respiratory viruses identified by multiplex PCR (e.g., RSV, HMPV, HRV, and HPIVs), affirming the reliability of both approaches (Fig. 4D). Beyond these common respiratory viruses, metatranscriptomic analysis revealed a broad spectrum of additional viral families, including *Papillomaviridae*, *Hepadnaviridae*, *Aspiviridae*, *Closteroviridae*, *Herpesviridae*, *Betaflexiviridae*, *Alphaflexiviridae*, *Virgaviridae*, *Endornaviridae*, and *Hafunaviridae*, reflecting the virome complexity present in pediatric respiratory samples. Comparative analysis of the top 15 most abundant viral families further revealed group-specific viral signatures. For instance, *Pneumoviridae* and *Herpesviridae* were enriched in PG samples, while *Virgaviridae* and *Hafunaviridae* were more prominent in NG samples (Fig. 4E, Supplementary Table S2).

Differential enrichment of respiratory microbiota across etiological groups and anatomical sites

To further explore the microbial composition associated with respiratory tract infections, we performed a comparative analysis of the top 10 most abundant bacterial genera identified across all

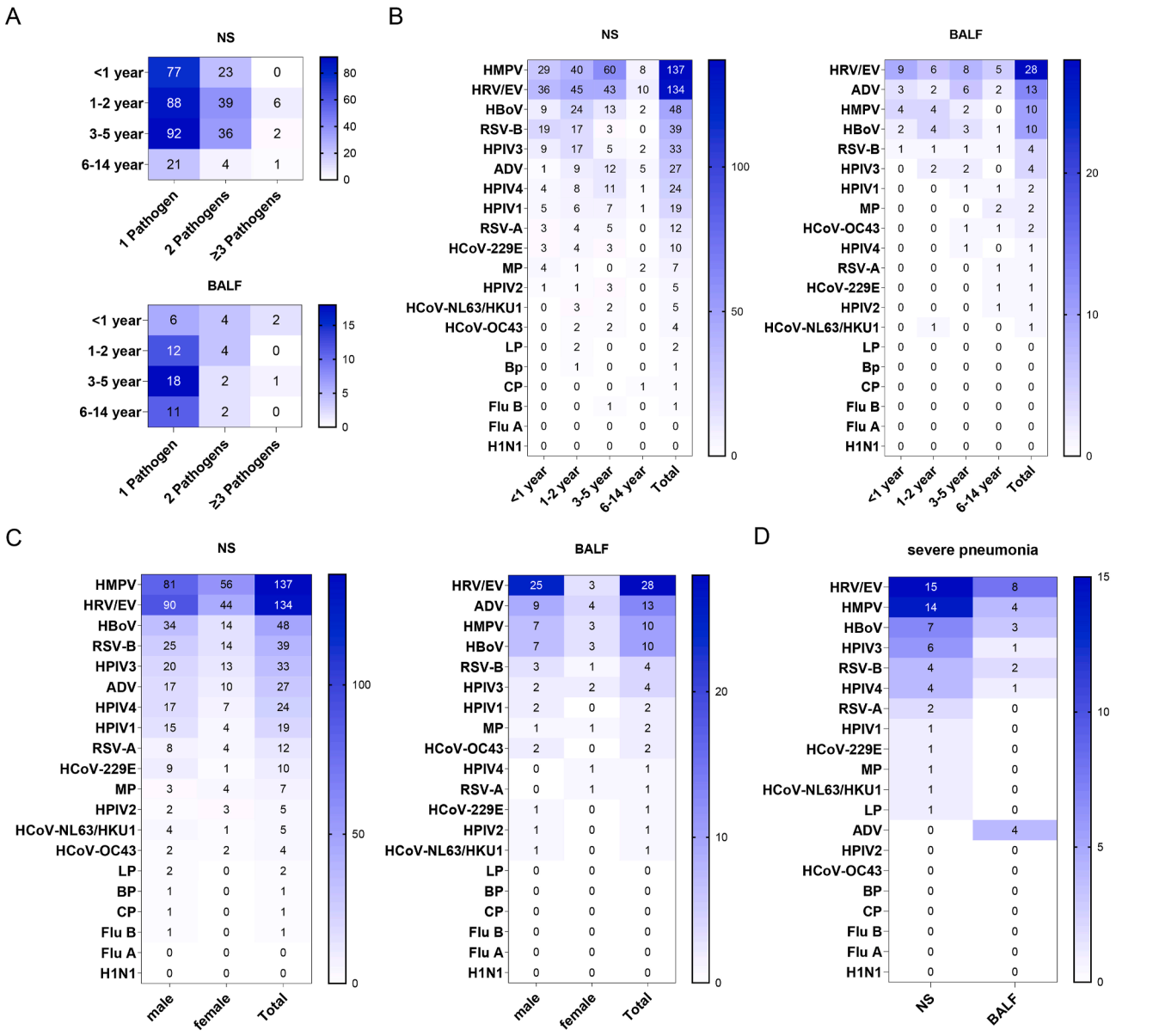

Fig. 2. Distribution and correlations of respiratory pathogens in pediatric pneumonia cohort. **A** Correlation between age and pathogen detected in swabs and BALF samples. **B** Age distribution of respiratory pathogens in pediatric patients. **C** Gender distribution of respiratory pathogens in pediatric patients. **D** Distributions of pathogens from pediatric patients with severe pneumonia.

metatranscriptomic datasets. These included *Veillonella*, *Sphingomonas*, *Streptococcus*, *Pseudomonas*, *Delftia*, *Moraxella*, *Propionibacterium*, *Prevotella*, *Haemophilus*, and *Capnocytophaga* (Fig. 5A, Supplementary Table S3). Notably, *Pseudomonas* was detected in both PG and NG groups; however, its relative abundance was significantly higher in the NG group ($P < 0.05$). Species-level annotation indicated that the *Pseudomonas* reads primarily corresponded to clinically common pathogenic lineages (Fig. 5B). We next investigated differences in microbial distribution between the upper and lower respiratory tracts. *Veillonella*, *Streptococcus*, *Prevotella*, and *Capnocytophaga* were predominantly enriched in NS samples, representing the upper respiratory tract, while *Pseudomonas*, *Delftia*, and *Propionibacterium* were more abundant in BALF samples, representing the lower respiratory tract (Fig. 5C). These findings highlight distinct microbial ecological niches within the respiratory tract and suggest anatomical site-specific microbial colonization or infection patterns. The observed enrichment of *Pseudomonas* in pathogen-negative patients underscores the need to consider non-canonical or fastidious bacterial pathogens in routine diagnostics. Furthermore, the spatial heterogeneity of the respiratory microbiome emphasizes the importance of sampling site selection in clinical diagnosis and research, which may influence pathogen detection sensitivity and the interpretation of microbial involvement in disease pathogenesis.

Detection of antibiotic resistance genes in ARTI patients

Antimicrobial resistance (AMR) is recognized as an urgent and escalating threat to global public health by international health authorities, and surveillance of resistance determinants is critical for informing treatment strategies and mitigating its impact. To investigate the prevalence of AMR in pediatric patients with ARTIs, we profiled antibiotic resistance genes (ARGs) by aligning metatranscriptomic sequencing reads to the Comprehensive Antibiotic Resistance Database (CARD). A total of eight ARGs were detected across the study groups. Specifically, *lnuC*, *ermB*, *tetM*, *mel*, and c*fxA* were identified in the pathogen-positive group (PG), while *ermB* and *cfxA3* were detected in NG group. In BALF-derived samples, *aph(6)-Id* was uniquely identified

A

Pathogens in nasopharyngeal swabs	HMPV	HRV/EV	HBoV	RSV-B	HPIV3	ADV	HPIV4	HPIV1	RSV-A	229E	MP	HPIV2	NL63/HKU1	OC43	LP	BP	CP	Flu B	Flu A	H1N1	Positive rate(%)
HMPV	137	13	15	0	6	0	1	6	1	6	0	4	2	2	0	0	0	0	0	0	27.13
HRV/EV		134	8	3	8	6	7	6	0	2	1	2	0	0	0	0	0	0	0	0	26.53
HBoV			48	3	1	2	0	1	2	1	0	0	1	0	0	1	0	0	0	0	9.5
RSV-B				39	0	1	0	0	0	1	4	0	0	0	0	0	0	0	0	0	7.72
HPIV3					33	1	0	0	1	0	0	0	0	0	1	0	0	0	0	0	6.53
HAdV						27	2	2	0	0	1	0	0	0	1	0	0	0	0	0	5.35
HPIV4							24	0	0	0	0	0	0	1	0	0	0	0	0	0	4.75
HPIV1								19	0	0	0	0	2	0	0	0	0	0	0	0	3.76
RSV-A									12	0	0	0	0	0	0	0	0	0	0	0	2.38
HCoV-229E										10	0	0	0	1	0	0	0	0	0	0	1.98
MP											7	0	0	0	0	0	0	0	0	0	1.39
HPIV2												5	0	0	0	0	0	0	0	0	0.99
HCoV-NL63/HKU1													5	0	0	0	0	0	0	0	0.99
HCoV-OC43														4	0	0	0	0	0	0	0.79
LP															2	0	0	0	0	0	0.4
BP																1	0	0	0	0	0.2
CP																	1	0	0	0	0.2
FluB																		1	0	0	0.2
FluA																			0	0	0
H1N1																				0	0
Single infection	86	82	16	28	17	14	14	4	9	1	1	0	1	2	1	0	1	1	0	0	71.47
Co-infection	51	52	32	11	16	13	10	15	3	9	6	5	4	2	1	1	0	0	0	0	28.53

B

Pathogens in bronchoalveolar lavage fluid	HRV/EV	ADV	HMPV	HBoV	RSV-B	HPIV3	HPIV1	MP	OC43	HPIV4	RSV-A	229E	HPIV2	NL63/HKU1	BP	LP	CP	Flu A	Flu B	H1N1	Positive rate(%)
HRV/EV	28	3	3	4	1	0	2	0	0	0	0	1	0	0	0	0	0	0	0	0	32.94
HAdV		13	0	0	0	0	0	0	0	0	0	0	0	0	0	0	0	0	0	0	15.29
HMPV			10	3	0	0	0	0	0	0	0	0	0	1	0	0	0	0	0	0	11.76
HBoV				10	0	0	1	0	0	0	0	0	0	0	0	0	0	0	0	0	11.76
RSV-B					4	0	1	0	0	0	0	0	0	0	0	0	0	0	0	0	4.71
HPIV3						4	0	0	0	0	0	0	0	0	0	0	0	0	0	0	4.71
HPIV1							2	0	0	0	0	0	0	0	0	0	0	0	0	0	2.35
MP								2	0	0	1	0	0	0	0	0	0	0	0	0	2.35
HCoV-OC43									2	0	0	0	0	0	0	0	0	0	0	0	2.35
HPIV4										1	0	0	0	0	0	0	0	0	0	0	1.18
RSV-A											1	0	0	0	0	0	0	0	0	0	1.18
HCoV-229E												1	0	0	0	0	0	0	0	0	1.18
HPIV2													1	0	0	0	0	0	0	0	1.18
HCoV-NL63/HKU1														1	0	0	0	0	0	0	1.18
BP															0	0	0	0	0	0	0
LP																0	0	0	0	0	0
CP																	0	0	0	0	0
FluA																		0	0	0	0
FluB																			0	0	0
H1N1																				0	0
Single infection	17	10	4	4	3	4	0	1	2	1	0	0	0	0	0	0	0	0	0	0	74.19
Co-infection	11	3	6	6	1	0	2	1	0	0	1	1	1	1	0	0	0	0	0	0	25.81

Fig. 3. Summary of respiratory pathogen distribution in 514 children diagnosed with acute respiratory tract infections (ARTI), based on multiplex PCR analysis of nasopharyngeal swabs (**A**) and bronchoalveolar lavage fluid (BALF) samples (**B**). HMPV, human metapneumovirus; HRV/EV, human rhinovirus/enterovirus; HBoV, human bocavirus; RSV-B, respiratory syncytial virus B; HPIV3, human parainfluenza virus 3; HAdV, human adenovirus; HPIV4, human parainfluenza virus 4; HPIV1, human parainfluenza virus 1; RSV-A, respiratory syncytial virus A; HCoV-229E, human coronavirus 229E; MP, *Mycoplasma pneumoniae*; HPIV2, human parainfluenza virus 2; HCoV-NL63/HKU1, human coronavirus NL63/HKU1; HCoV-OC43, human coronavirus OC43; HCoV-229E, human coronavirus 229E; LP, *Legionella pneumophila*; BP, *Bordetella pertussis*; CP, *Chlamydia pneumoniae*; FluB, influenza virus B; FluA, influenza virus A; H1N1, influenza A H1N1 virus.

in the BALF-pathogen-positive group (BPG), and *rsmA* was detected in the BALF-pathogen-negative group (BNG). Notably, no resistance genes were found in samples from healthy controls (Fig. 6). These findings underscore the presence of diverse ARGs in respiratory specimens from ARTI patients, particularly among those with detectable pathogens or lower respiratory tract involvement.

Microbial composition differences between mild and severe respiratory infections

To further investigate the relationship between respiratory pathogens and disease severity, we compared microbial profiles between mild and severe cases. Consistent with statistical analyses, no significant

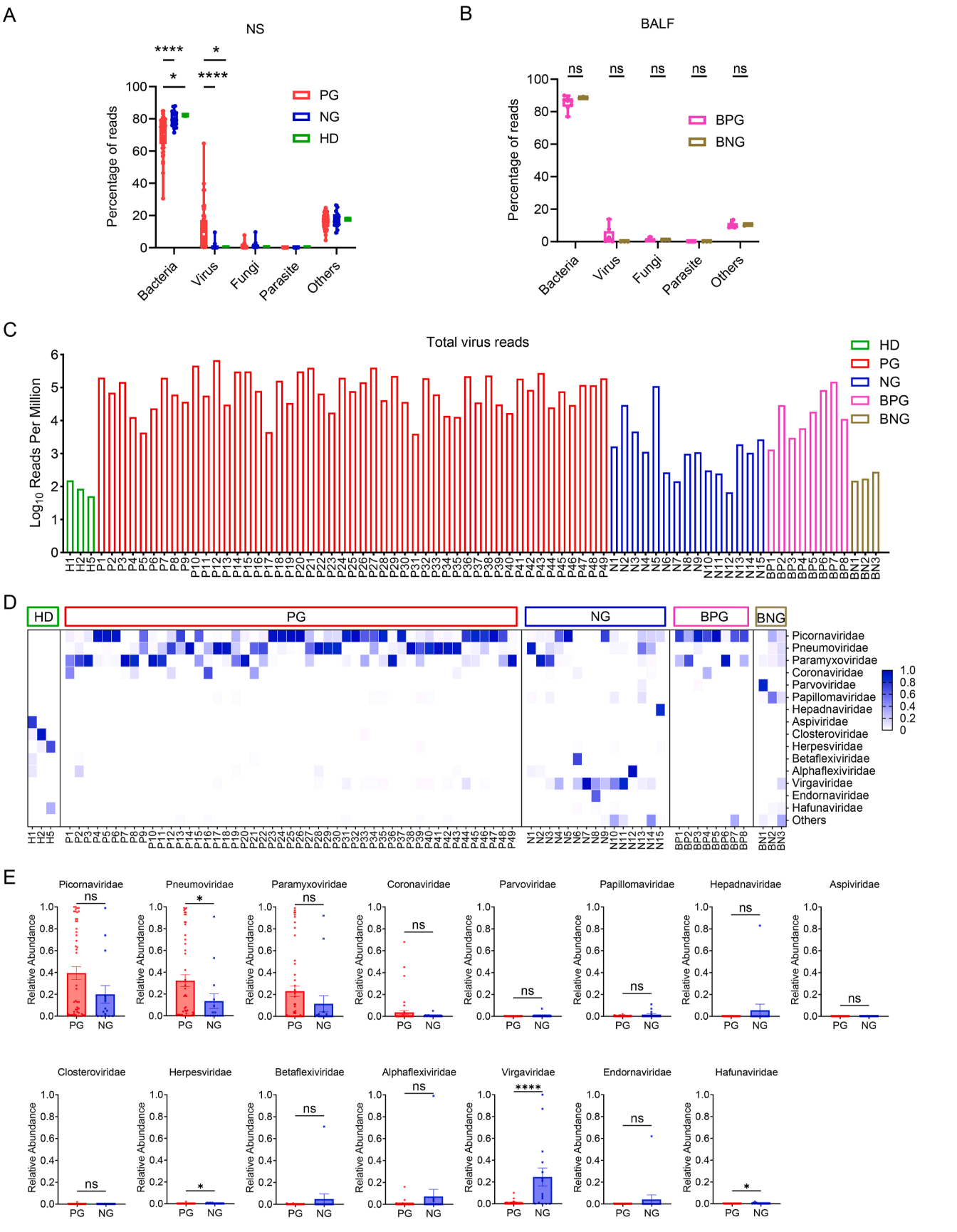

(caption on next page)

differences were observed between mild and severe upper-airway samples. However, in lower-airway (BALF) samples from severe cases, bacterial read proportions were significantly higher than in upper-airway samples from both mild and severe patients, while viral read proportions were significantly lower than those observed in mild upper-airway samples (Fig. 7A). Virome comparison showed that the top four viral families, *Picornaviridae*, *Pneumoviridae*, *Paramyxoviridae*, and *Coronaviridae* were consistently detected in both mild and severe cases, suggesting a common viral etiology across clinical spectrums (Fig. 7B, Supplementary Table S4). Statistical analysis also indicated no significant differences in the relative abundance of these dominant viral families between mild and severe respiratory infections cases (Fig. 5D). Microbiome profiling further revealed a shared set of top 10 bacterial genera between mild and severe cases (Fig. 5C, Supplementary Table S5), though with marked variations in relative abundance. Notably, *Pseudomonas* was significantly enriched in severe cases, whereas *Veillonella* was more abundant in mild infections (Fig. 5E). These findings indicate that while the spectrum of microbial colonization is broadly similar, specific taxa may be associated with disease progression and severity.

DISCUSSION

This study provides an integrated etiological and microbiological characterization of pediatric ARTIs by combining multiplex PCR with metatranscriptomic sequencing. Through parallel analysis of upper (NS) and lower (BALF) airway samples, our findings refine the understanding of pathogen distribution, highlight microbial signatures associated with undiagnosed infections, and underscore the complementary value of unbiased sequencing in routine diagnostics. To contextualize our findings, we compared them with prior studies on pediatric ARTIs. Earlier work has typically focused on either upper-airway or BALF microbiota, or relied solely on PCR detection, providing an incomplete view of the respiratory microbial landscape. By integrating multiplex PCR and metatranscriptomic sequencing across both airway levels in the same cohort, our study offers a more comprehensive assessment, enabling simultaneous analysis of disease severity, pathogen-negative cases, and antibiotic resistance gene profiles.

Consistent with previous reports, we observed that HMPV, HRV, and HBoV remain predominant viral pathogens in our cohort (Principi et al., 2013; Brealey et al., 2021). An unexpected observation was the markedly low influenza virus detection, which aligns with recent post-COVID-19 circulation patterns showing sustained suppression of seasonal influenza. Phylogenetic analyses of major viruses revealed subtype distributions (RSV-BA.9, HBoV1, HMPV-B) consistent with locally and globally circulating lineages, while adenoviruses demonstrated broader genotypic heterogeneity, reflecting their endemic, multi-lineage transmission dynamics. These results emphasize that viral evolutionary patterns differ substantially: epidemic-prone viruses such as RSV and HMPV exhibit compact, outbreak-like phylogenies, whereas HRV/EV show greater diversity, consistent with continuous circulation and detection in both symptomatic and healthy children.

A central finding of this study is the distinct microbial profile of PCR-negative ARTIs. While PCR-positive pools were dominated by viral transcripts, PCR-negative pools showed a clear shift toward bacterial abundance, suggesting that some undiagnosed cases may involve bacterial etiologies missed by routine PCR panels. Several observations support that the *Pseudomonas* enrichment in pathogen-negative samples reflects true infection rather than contamination: no *Pseudomonas* transcripts were detected in parallel healthy controls; its read abundance far exceeded typical environmental background levels; and enrichment was mainly observed in BALF, consistent with the pathogenic behavior of *Pseudomonas* in the lower airway. These findings indicate that *Pseudomonas* likely represents a meaningful bacterial signal in PCR-negative ARTIs.

Differences between mild and severe infections further illustrate how disease severity shapes the airway microbiome. Although the major viral families were present in both groups, severe cases exhibited a shift toward bacteria-rich profiles, with a notable enrichment of *Pseudomonas*, whereas mild infections showed relatively higher viral contributions. This pattern is consistent with previous reports linking bacterial overgrowth or airway dysbiosis, including opportunistic pathogens, to more severe clinical presentations (Faner et al., 2017; Lin et al., 2025). Although causation cannot be established from pooled metatranscriptomic data, these observations underscore the need for future individual-level sequencing to clarify whether specific taxa influence disease progression or reflect secondary bacterial involvement.

Low-abundance plant-associated viral sequences were also detected in some datasets. These sequences, such as pepper mild mottle virus and citrus psorosis virus, have been widely reported in respiratory and gastrointestinal metagenomic studies and likely originate from dietary intake, plant-derived particulates, or environmental exposures rather than representing true respiratory infection (Worp et al., 2025). Their extremely low abundance and absence of known pathogenicity support this interpretation.

Fungal and parasitic organisms were also examined in the metatranscriptomic data; however, only extremely low-abundance reads were detected, comparable to background levels and similar to healthy controls. None met the predefined thresholds for pathogen identification, indicating that fungi and parasites did not contribute to the ARTIs in our cohort (Elbehiry and Abalkhail, 2025).

Host immune-microbiome associations were explored; however, no reproducible or biologically interpretable patterns emerged. The lack of consistent associations is likely due to heterogeneous disease stages at sampling, substantial age-related immunological variability in pediatric patients, and the inherent limitations of a pooled sequencing strategy, which reduces individual-level resolution. To avoid over interpretation, immune-microbiome correlations were not included in the final analysis and are now explicitly acknowledged as a limitation (Doxey et al., 2025).

As for the pooling strategy considerations, the use of eight-sample pooling in this study may influence quantitative interpretation. Pooling can dilute low-abundance taxa, obscure inter-individual variability, and allow high-biomass samples to disproportionately shape pooled profiles. Because individual microbial signals cannot be reconstructed, correlations with patient-level clinical features are also limited. This approach was adopted due to the large cohort size and the high sequencing depth required for metatranscriptomic analysis, and represents a commonly used strategy in exploratory mNGS studies.

This study highlights the diagnostic limitations of conventional multiplex PCR compared to metatranscriptomic sequencing in pediatric respiratory infections. Metatranscriptomic sequencing can

Fig. 4. Viral profiles in ARTI patients and healthy controls. **A, B** Overview of reads mapping to viruses, bacteria, and other microbes in nasopharyngeal swabs (**A,** NS) and bronchoalveolar lavage fluid (**B,** BALF) samples of ARTI patients. Data distribution was assessed using the Shapiro-Wilk normality test. Differences between groups were evaluated using Two-way ANOVA followed by Tukey's multiple comparisons test. **C** Total viral read counts across 75 respiratory tract specimen pools from ARTI patients and healthy donors. Read counts were normalized as reads per million (RPM). **D** Heatmap showing the relative abundance of viral families across all specimen pools. The top 15 viral families were ranked by average abundance in samples from both ARTI patients and healthy controls. **E** Comparative analysis of the relative abundance of the top 15 viral families between pathogen-positive (PG) and pathogen-negative (NG) groups. Data normality was assessed using the Shapiro–Wilk test. Mann-Whitney test was performed for comparison. Group definitions: HD, healthy donor; PG, pathogen-positive group (PCR-confirmed infection); NG, pathogen-negative group (no pathogen detected); BPG, BALF samples from the pathogen-positive group; BNG, BALF samples from the pathogen-negative group. Statistical significance was defined as $P < 0.05$. Significance levels: $P < 0.05$ (*), $P < 0.0001$ (****); ns, not significant.

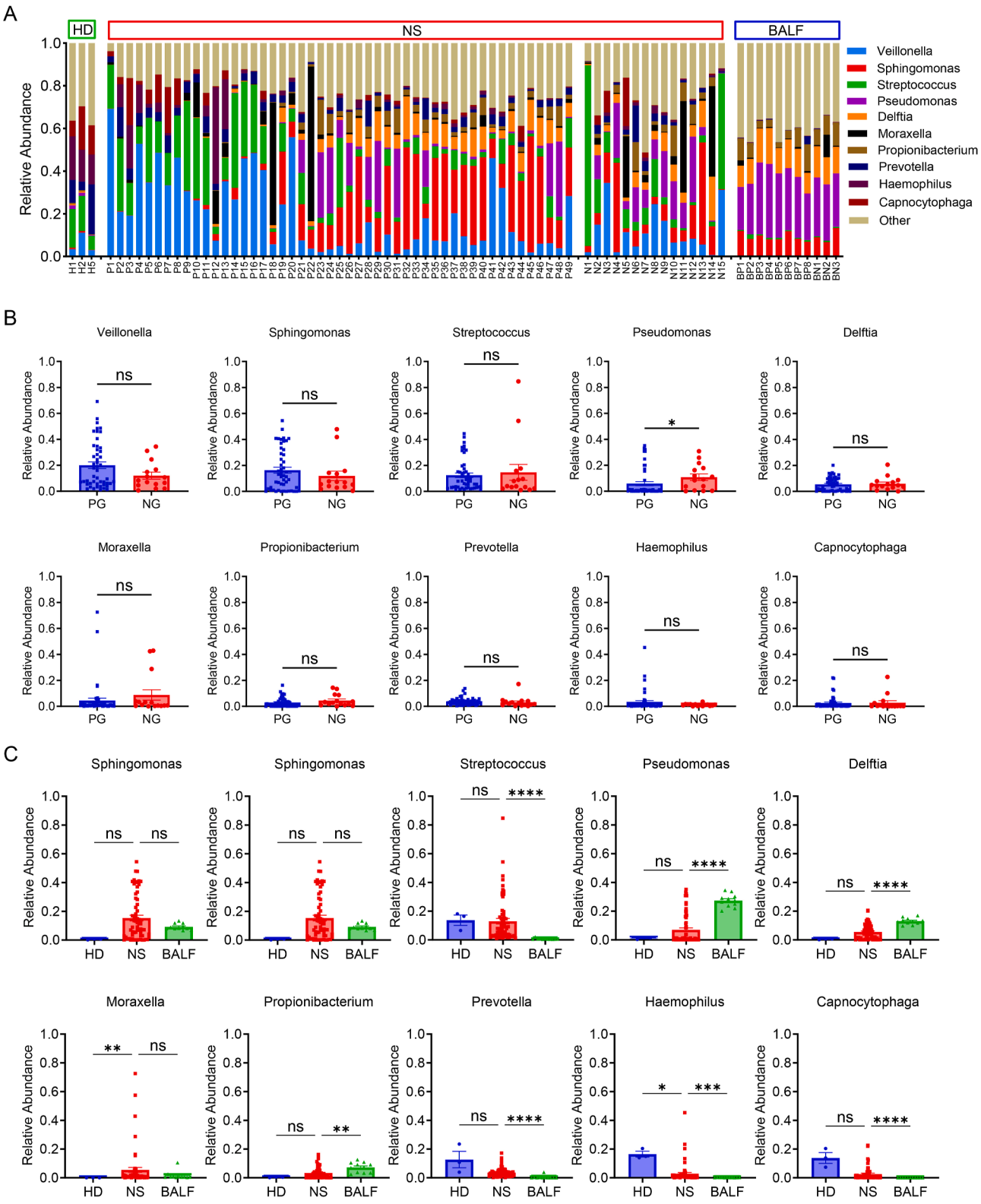

Fig. 5. Microbiome profiles in pediatric ARTI patients and healthy controls. **A** Bar plot showing the relative abundance of the top 10 bacterial genera across all samples. The genera were ranked based on their average abundance in different clinical groups. **B** Comparative analysis of the relative abundance of the top 10 bacterial genera between pathogen-positive (PG) and pathogen-negative (NG) groups. Data normality was assessed using the Shapiro-Wilk test. Mann-Whitney test was performed for comparison. **C** Comparative analysis of microbial composition between upper respiratory tract (nasopharyngeal swabs) and lower respiratory tract (BALF) samples. Data normality was assessed using the Shapiro-Wilk test. Group comparisons were performed using the Kruskal-Wallis test with Dunn's multiple comparisons test. Group abbreviations: HD, healthy donor; NS, nasopharyngeal swab; BALF, bronchoalveolar lavage fluid. A *P*-value <0.05 was considered statistically significant. Significance levels: $P < 0.05$ (*), $P < 0.01$ (**), $P < 0.001$ (***), $P < 0.0001$ (****); ns, not significant.

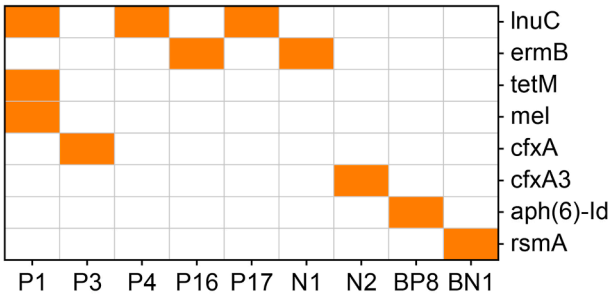

Fig. 6. Heatmap of antibiotic resistance gene profiles across 75 respiratory tract sample pools. Antibiotic resistance genes (ARGs) were identified based on sequence identity > 80% and target gene coverage > 60%. The heatmap illustrates the relative abundance and distribution of ARGs across all sample pools.

comprehensively reveal the coexistence of bacteria, viruses, fungi, rare pathogens, and unknown pathogens. It also helps avoid the misuse of broad-spectrum antibiotics and promotes their targeted use, thereby providing a basis for formulating precise anti-infection treatment plans and should be promoted in clinical diagnostics. However, it faces challenges such as high testing costs, the lack of internationally standardized operating procedures, and lengthy reporting times. Future efforts should focus on developing rapid and clinically applicable metagenomic tools for real-time pathogen and resistance gene detection. The development of automated library preparation equipment, integrated analysis software, and AI-assisted interpretation will be key to improving diagnostic specificity and achieving clinical translation (Gu et al., 2019).

In addition, we reviewed antibiotic resistance gene (ARG) profiles in the context of local clinical data. Although routine culture-based antimicrobial susceptibility testing was not available for most outpatient cases, the dominant ARGs detected in our metatranscriptomic analysis, such as *ermB*, *tetM* and *cfxA*, were consistent with resistance patterns reported in our hospital's pediatric surveillance data. This concordance suggests that the detected ARGs reflect the local resistance ecology despite the absence of individual-level AST correlation (Mai et al., 2023). These findings support the need to update current diagnostic strategies, improve antimicrobial use, and advance precision care in pediatric respiratory infections.

CONCLUSIONS

This study comprehensively profiled respiratory pathogens and microbiota in pediatric ARTI patients using multiplex PCR and metatranscriptomic sequencing. We identified distinct microbial signatures between PG and -NG groups, upper and lower airways, and mild versus severe cases. Key taxa and resistance genes were associated with disease severity. These findings enhance our understanding of pediatric respiratory infections and support more precise diagnostic and therapeutic strategies.

MATERIALS AND METHODS

Study design and patients enrolled in this study

Between December 2020 and July 2021, respiratory samples were collected from 514 hospitalized pediatric patients diagnosed with ARTIs. A total of 505 nasopharyngeal swab (NS) and 85 bronchoalveolar lavage fluid (BALF) samples were obtained. All eligible children admitted with a clinical diagnosis of ARTI were screened for inclusion. Initial pathogen detection was performed using a 22-target multiplex PCR assay (RespiFinder 2SMART assay, Shanghai GeneoDx Biotech, China) to identify both viral and bacterial agents. Patients were classified into two groups based on PCR findings: PG group, with a defined infectious agent, and NG group, with no detectable pathogen. NS and BALF samples from each group were randomly pooled in sets of eight and subjected to next-generation sequencing (NGS) for further etiological investigation. Demographic and clinical outcome data were extracted from electronic medical records. Phylogenetic analysis was subsequently conducted on the five most frequently detected viruses, based on specific gene targets.

Multiplex PCR detection of respiratory pathogens

Total nucleic acids (DNA and RNA) were extracted from 200 μL of NS or BALF samples using a magnetic bead-based nucleic acid extraction kit (Zybio, China), following the manufacturer's protocol. Elution was performed in 60 μL of buffer. Pathogen detection was conducted using the RespiFinder 2SMART assay (Shanghai GeneoDx Biotech), targeting 22 common respiratory pathogens, including HAdV, HBoV, common human coronaviruses (HCoV-229E/OC43/NL63/HKU1), HMPV, Influenza A (Flu A) and Influenza virus B (Flu B), Influenza A H1N1 virus (H1N1pdm09), HPIV1/2/3/4, HRV/EV, RSV-A and RSV-B, *Bordetella pertussis* (BP), *Chlamydia pneumoniae* (CP), *Legionella pneumophila* (LP), and *Mycoplasma pneumoniae* (MP). Internal, amplification, and positive controls were included in each assay run.

Metatranscriptomic library preparation and sequencing

Viral nucleic acid was extracted using the QIAamp Viral RNA Mini Kit (Qiagen, Germany) according to the manufacturer's protocol, and quantified with the Qubit RNA High Sensitivity Assay on a Qubit 3.0 Fluorometer (Life Technologies, USA). RNA samples were reverse transcribed into cDNA and amplified by PCR following pre-processing, using the IDseq Library Preparation Kit (Vision Medicals, China). Purification of RNA and PCR products was performed using RNAClean XP and AMPure XP beads (Beckman Coulter, USA), respectively. PCR products were quantified using the Qubit dsDNA High Sensitivity Assay, and sequencing libraries were constructed via a transposase-based method (Vision Medicals, China). Pooled libraries were sequenced on the Illumina NextSeq 550 platform, generating 75 bp single-end reads. A negative control was included in each sequencing run for quality assessment. Healthy control samples processed alongside patient samples showed no detectable *Pseudomonas* transcripts, supporting the specificity of patient-derived microbial signals.

Analysis of sequencing data

Raw reads generated from the Illumina NextSeq 550 platform were first processed using the in-house IDseq pipeline (Vision Medicals, China) (Zhan et al., 2021). Low-quality reads, short fragments, and adapter contaminants were removed using default parameters. Host-derived reads were filtered by mapping to the human reference genome (hg19). The remaining non-host reads were taxonomically classified by aligning to curated local microbial genome databases, including viruses, bacteria, fungi, and parasites. Low-abundance viral and microbial taxa were retained for completeness. Plant-associated viral sequences were interpreted as environmental or dietary exposures rather than indicators of infection, consistent with prior respiratory metagenomic literature (Zhong et al., 2021). Microbiome profiling and antimicrobial resistance gene (ARG) annotation were subsequently performed using the CLC Genomics Workbench (version 22.0.1, Qiagen, Germany) with either custom reference databases or the Comprehensive Antibiotic Resistance Database (CARD) (Alcock et al., 2019). Standard microbial reference genomes were retrieved via the CLC Microbial Genomics Module. Sequencing data were subjected to quality control using a threshold Phred quality score cutoff of 0.05, a maximum of two ambiguous nucleotides, and a minimum read length of 35 nt. Taxonomic profiling was performed using the "QC and Taxonomic Profiling" workflow. Clean reads were mapped to CARD for identification of ARGs,

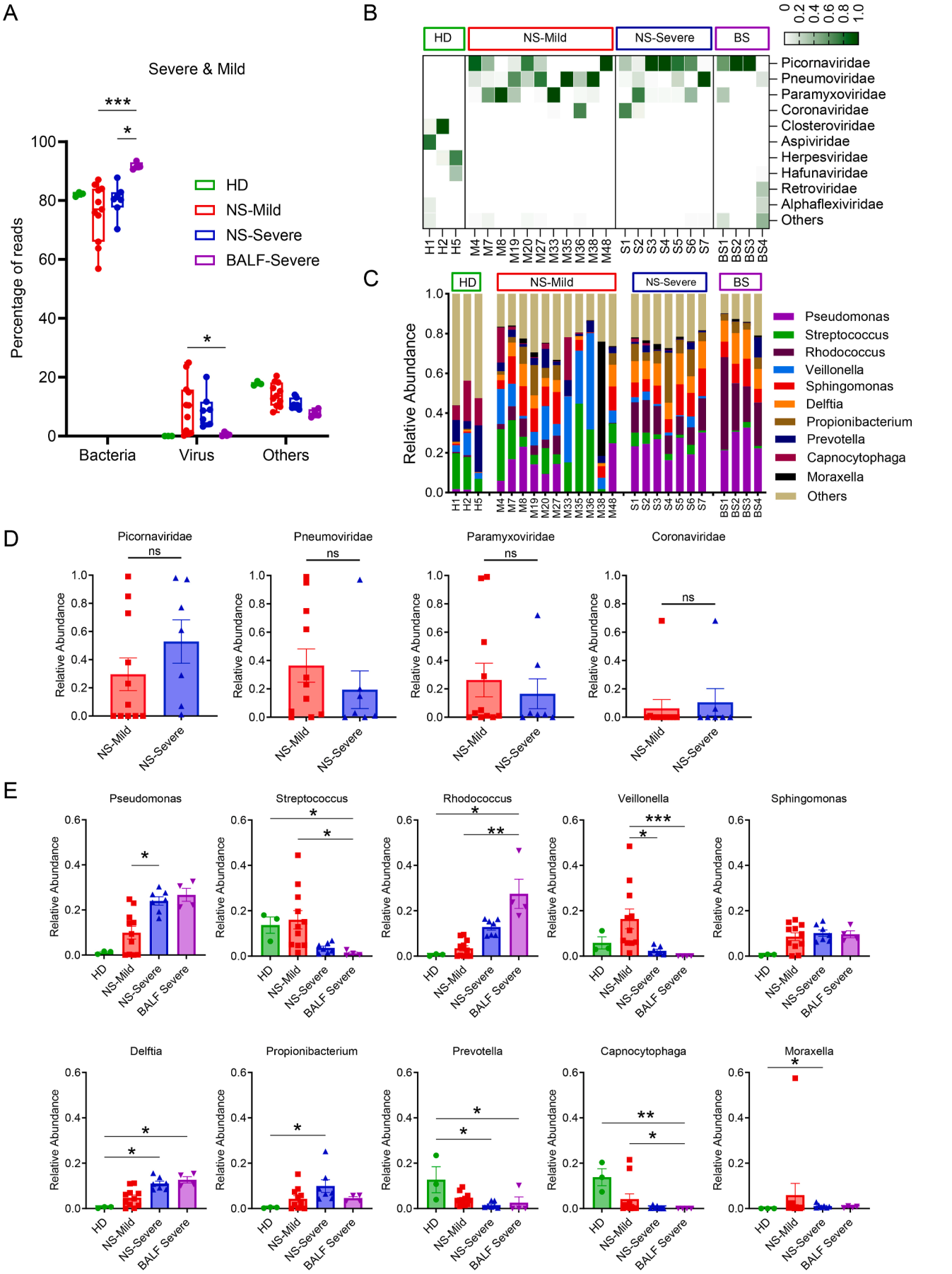

(caption on next page)

Fig. 7. Comparison of respiratory microbiome profiles between mild and severe pneumonia cases. **A** Distribution of sequencing reads mapped to viruses, bacteria, and other microbes in nasopharyngeal swabs and BALF samples from patients with mild or severe pneumonia. Normality of data distribution was assessed using the Shapiro-Wilk test. Group differences were evaluated using Two-way ANOVA followed by Tukey's multiple comparisons test. **B** Heatmap showing the relative abundance of the top 10 viral families in each group. **C** Bar plot of the relative abundance of the top 10 bacterial genera across mild and severe cases. **D** Differential abundance analysis of the top four viral families between mild and severe pneumonia cases. Data normality was assessed using the Shapiro-Wilk test. Mann-Whitney test was performed for comparison. **E** Differential abundance analysis of the top 10 microbial genera between mild and severe cases. Normality of data distribution was assessed using the Shapiro-Wilk test. Group differences were evaluated using the Kruskal-Wallis test followed by Dunn's multiple comparisons test. Group abbreviations: HD, healthy donor; NS-mild, nasopharyngeal swab from patients with mild respiratory symptoms; NS-severe, nasopharyngeal swab from patients with severe pneumonia; BS, bronchoalveolar lavage fluid from patients with severe pneumonia. A *P*-value <0.05 was considered statistically significant. Significance levels are indicated as follows: $P < 0.05$ (*), $P < 0.01$ (**), $P < 0.001$ (***); ns, not significant.

with genes retained if they had ≥ 60% sequence identity and ≥ 30% query coverage.

Phylogenetic analysis

To analyze the phylogenetic relationships of predominant respiratory viruses detected in this study, viral nucleotide sequences were aligned to GenBank references. Phylogenetic trees were inferred using the Neighbor-Joining method in MEGA (v5.0) with 1000 bootstrap replicates. All other parameters were set to default.

Statistical analysis

Statistical analyses were conducted using GraphPad Prism version 8.0. Differences between groups were assessed by Student's *t*-test, one-way ANOVA or two-way ANOVA, as appropriate. Statistical significance was defined as $P < 0.05$. Significance levels are indicated as follows: *, $P \leq 0.05$, **, $P \leq 0.01$, ***, $P \leq 0.001$, and ****, $P \leq 0.0001$.

DATA AVAILABILITY

Partial genome sequences generated in this study are available in the Science Data Bank (https://doi.org/10.57760/sciencedb.36281) and have been deposited in GenBank under accession numbers OQ382964–OQ383026, OQ383033–OQ383129, and OQ408547–OQ408617. Raw sequencing data are available in the Science Data Bank (https://doi.org/10.57760/sciencedb.36281) and have been submitted to the Genome Sequence Archive (GSA) of the National Genomics Data Center, China National Center for Bioinformation/Beijing Institute of Genomics, Chinese Academy of Sciences (accession number CRA030475), and are publicly accessible at https://ngdc.cncb.ac.cn/gsa. Exploratory analyses of immune-microbiome correlations were performed but did not yield consistent patterns due to inter-individual heterogeneity and pooled-sample constraints. Thus, these results were not included to avoid over interpretation.

ETHICS STATEMENT

The study was conducted in full compliance with ethical guidelines for human subject research, as approved by the Ethics Committees of the First Affiliated Hospital of Guangzhou Medical University (2020-085) and the Guangzhou Women and Children's Medical Center. Written informed consent was obtained from the parents or legal guardians of all participants.

AUTHOR CONTRIBUTIONS

Peilan Wei: investigation, methodology, data curation, writing-original draft. Lu Zhang: data curation, formal analysis, methodology. Qingtao Hu: data curation, formal analysis, software. Airu Zhu: data curation, formal analysis, resources. Zhen Zhuang: methodology, validation, visualization. Zhaoyong Zhang: formal analysis, resources. Shengnan Zhang: formal analysis, resources. Jiantao Chen: formal analysis, resources. Xinyi Xiong: formal analysis, resources. Bin Qu: formal analysis, resources. Yuanyuan Zhang: investigation, methodology. Lei Chen: investigation, methodology. Zhiwei Xu: investigation, methodology. Zhao Chen: investigation, methodology. Qier Zhong: investigation, methodology. Xindan Xing: investigation, methodology. Xinxin Li: investigation, methodology. Jingjing Gao: investigation, methodology. Yifang He: investigation, methodology. Guifei Xie: investigation, methodology. Juan Shang: investigation, methodology. Xiaoke Guo: investigation, methodology. Jiaxin Jiang: investigation, methodology. Yongxia Shi: investigation, methodology. Jingxian Zhao: conceptualization, resources, writing-review, editing and funding acquisition. Yanqun Wang: conceptualization, resources, writing-review, editing and funding acquisition. Jincun Zhao: conceptualization, resources, writing-review, editing and funding acquisition. Yingkang Jin: conceptualization, funding acquisition, writing and supervision. All authors have read and agreed to the final version of the manuscript.

CONFLICT OF INTEREST

The authors declare that they have no conflict of interest.

ACKNOWLEDGEMENTS

This project was supported by grants from the National Key Research and Development Program of China (2024YFC2310205 to L.Z.), the National Natural Science Foundation of China (82025001, 82495200 and 82495203 to J.C.Z., 92369113 and 82172240 to Y.Q.W.), the Guangdong Medical Technology Research Foundation (B2022233 to Y.K.J.), the Guangzhou National Laboratory and State Key Laboratory of Respiratory Disease (GZNL2024B01001 to Y.Q.W., and GZNL2023A01004 to Y.K.J.), the Guangdong Basic and Applied Research Projects (2023B1515020040 to Y.Q.W.), the State Key Laboratory of Respiratory Disease (SKLRD-Z-202411 to L.Z., SKLRD-OP-202309 to Y.Q.W), the Science and Technology Planning Project of Guangzhou City (2024A03J1230 to J.C.Z., 2025B04J0006 to L.Z.), and the Science and Technology Project of General Administration of Customs, P.R. China (2025HK221, 2023HK065 to L.Z.). We thank the Biobank for Respiratory Disease in the National Clinical Research Center for Respiratory Disease (BRD-NCRCRD, Guangzhou, China).

APPENDIX A. SUPPLEMENTARY DATA

Supplementary data to this article can be found online at https://doi.org/10.1016/j.virs.2026.02.001.

REFERENCES

Alcock, B.P., Raphenya, A.R., Lau, T.T.Y., Tsang, K.K., Bouchard, M., Edalatmand, A., Huynh, W., Nguyen, A.-L.V., Cheng, A.A., Liu, S., Min, S.Y., Miroshnichenko, A., Tran, H.-K., Werfalli, R.E., Nasir, J.A., Oloni, M., Speicher, D.J., Florescu, A., Singh, B., Faltyn, M., Hernandez-Koutoucheva, A., Sharma, A.N., Bordeleau, E., Pawlowski, A.C., Zubyk, H.L., Dooley, D., Griffiths, E., Maguire, F., Winsor, G.L., Beiko, R.G., Brinkman, F.S.L., Hsiao, W.W.L., Domselaar, G.V., McArthur, A.G., 2019. Card 2020: antibiotic resistome surveillance with the comprehensive antibiotic resistance database. Nucleic Acids Res. 48, D517–D525.

Bai, Y., Hu, Y., Chen, X., Hu, L., Wu, K., Liang, S., Zheng, J., Gänzle, M.G., Chen, C., 2025. Comparative metagenome-associated analysis of gut microbiota and antibiotic resistance genes in acute gastrointestinal injury patients with the risk of in-hospital mortality. mSystems 10, e0144424.

Bradley, J.S., Byington, C.L., Shah, S.S., Alverson, B., Carter, E.R., Harrison, C., Kaplan, S. L., Mace, S.E., McCracken Jr., G.H., Moore, M.R., St Peter, S.D., Stockwell, J.A., Swanson, J.T., Pediatric Infectious Diseases, S., the Infectious Diseases Society of A, 2011. The management of community-acquired pneumonia in infants and children older than 3 months of age: clinical practice guidelines by the pediatric infectious diseases society and the infectious diseases society of America. Clin. Infect. Dis. 53, e25–e76.

Brealey, J.C., Leitão, H.G., Hofstede, T., Kalthoff, D.C., Guschanski, K., 2021. The oral microbiota of wild bears in Sweden reflects the history of antibiotic use by humans. Curr. Biol. 31, 4650–4658.

Candel, F.J., Salavert, M., Cantón, R., Del Pozo, J.L., Galán-Sánchez, F., Navarro, D., Rodríguez, A., Rodríguez, J.C., Rodríguez-Aguirregabiria, M., Suberviola, B., Zaragoza, R., 2024. The role of rapid multiplex molecular syndromic panels in the clinical management of infections in critically ill patients: an experts-opinion document. Crit. Care 28, 440.

Doxey, A.C., Abu Mazen, N., Homm, M., Chu, V., Hunjan, M., Lobb, B., Lee, S., Kurs-Lasky, M., Williams, J.V., MacDonald, W., Johnson, M., Hirota, J.A., Shaikh, N., 2025. Metatranscriptomic profiling reveals pathogen and host response signatures of pediatric acute sinusitis and upper respiratory infection. Genome Med. 17, 22.

Elbehiry, A., Abalkhail, A., 2025. Metagenomic next-generation sequencing in infectious diseases: clinical applications, translational challenges, and future directions. Diagnostics 15, 1991.

Faner, R., Sibila, O., Agustí, A., Bernasconi, E., Chalmers, J.D., Huffnagle, G.B., Manichanh, C., Molyneaux, P.L., Paredes, R., Pérez Brocal, V., Ponomarenko, J., Sethi, S., Dorca, J., Monsó, E., 2017. The microbiome in respiratory medicine: current challenges and future perspectives. Eur. Respir. J. 49, 1602086.

Galeeva, J.S., Fedorov, D.E., Starikova, E.V., Manolov, A.I., Pavlenko, A.V., Selezneva, O. V., Klimina, K.M., Veselovsky, V.A., Morozov, M.D., Yanushevich, O.O., Krikheli, N. I., Levchenko, O.V., Andreev, D.N., Sokolov, F.S., Fomenko, A.K., Devkota, M.K., Andreev, N.G., Zaborovskiy, A.V., Bely, P.A., Tsaregorodtsev, S.V., Evdokimov, V.V., Maev, I.V., Govorun, V.M., Ilina, E.N., 2024. Microbial signatures in COVID-19: distinguishing mild and severe disease via gut microbiota. Biomedicines 12, 996.

Gu, W., Miller, S., Chiu, C.Y., 2019. Clinical metagenomic next-generation sequencing for pathogen detection. Annu. Rev. Pathol. 14, 319–338.

Harris, M., Clark, J., Coote, N., Fletcher, P., Harnden, A., McKean, M., Thomson, A., 2011. British thoracic society guidelines for the management of community acquired pneumonia in children: update 2011. Thorax 66 (Suppl. 2), ii1–23.

Hou, M., Liu, G., Meng, C., Dong, L., Fang, Y., Wang, L., Wang, N., Cai, C., Wang, H., 2024. Circulation patterns and molecular characteristics of respiratory syncytial virus among hospitalized children in tianjin, China, before and during the COVID-19 pandemic (2017-2022). Virol. Sin. 39, 719–726.

Kelly, M.S., Shi, P., Boiditswe, S.C., Qin, E., Steenhoff, A.P., Mazhani, T., Patel, M.Z., Cunningham, C.K., Rawls, J.F., Luinstra, K., Gilchrist, J., Maciejewski, J., Hurst, J.H., Seed, P.C., Bulir, D., Smieja, M., 2025. Role of the upper airway microbiota in respiratory virus and bacterial pathobiont dynamics in the first year of life. Nat. Commun. 16, 5195.

Lin, Z., Jiang, Y., Liu, H., Yang, J., Yang, B., Zhang, K., Tang, P., Xiang, B., Sun, B., 2025. Airway microbiota and immunity associated with chronic obstructive pulmonary disease severity. J. Transl. Med. 23, 962.

Mai, W., Liu, Y., Meng, Q., Xu, J., Wu, J., 2023. Bacterial epidemiology and antimicrobial resistance profiles of respiratory specimens of children with pneumonia in Hainan, China. Infect. Drug Resist. 16, 249–261.

Man, W.H., de Steenhuijsen Piters, W.A., Bogaert, D., 2017. The microbiota of the respiratory tract: gatekeeper to respiratory health. Nat. Rev. Microbiol. 15, 259–270.

Principi, N., Bianchini, S., Baggi, E., Esposito, S., 2013. No evidence for the effectiveness of systemic corticosteroids in acute pharyngitis, community-acquired pneumonia and acute otitis media. Eur. J. Clin. Microbiol. Infect. Dis. 32, 151–160.

Um, S., Vang, D., Pin, P., Chau, D., 2023. Trends and determinants of acute respiratory infection symptoms among under-five children in Cambodia: analysis of 2000 to 2014 Cambodia demographic and health surveys. PLOS Glob Public Health 3, e0001440.

Wang, D., Duan, Y., He, L., Jiang, J., Xian, J., Yuan, K., Zhang, R., Zhang, H., Wang, J., Li, N., Huang, M., Hu, C., Lu, S., Luo, Z., Deng, T., Zhang, Z., Chen, B., Li, W., 2025. Altered microbiota of the lower respiratory tract and its association with COVID-19 severity analysed by metagenomics and metatranscriptomics. Commun. Biol. 8, 804.

Wang, Y., Zhu, N., Li, Y., Lu, R., Wang, H., Liu, G., Zou, X., Xie, Z., Tan, W., 2016. Metagenomic analysis of viral genetic diversity in respiratory samples from children with severe acute respiratory infection in China. Clin. Microbiol. Infect. 22, e451–e459.

Waskito, L.A., Rezkitha, Y.A.A., Vilaichone, R.K., Wibawa, I.D.N., Mustika, S., Sugihartono, T., Miftahussurur, M., 2022. Antimicrobial resistance profile by metagenomic and metatranscriptomic approach in clinical practice: opportunity and challenge. Antibiotics (Basel) 11, 654.

Worp, N., Nieuwenhuijse, D.F., Izquierdo-Lara, R.W., Schapendonk, C.M.E., Brinch, C., Jensen, E.E.B., Munk, P., Hendriksen, R.S., Aarestrup, F., Oude Munnink, B.B., Koopmans, M.P.G., de Graaf, M., 2025. Unveiling the global urban virome through wastewater metagenomics. Nat. Commun. 16, 10707.

Yang, S., Rothman, R.E., 2004. PCR-based diagnostics for infectious diseases: uses, limitations, and future applications in acute-care settings. Lancet Infect. Dis. 4, 337–348.

Zelasko, S., Swaney, M.H., Sandstrom, S., Lee, K.E., Dixon, J., Riley, C., Watson, L., Godfrey, J.J., Ledrowski, N., Rey, F., Safdar, N., Seroogy, C.M., Gern, J.E., Kalan, L., Currie, C., 2025. Early-life upper airway microbiota are associated with decreased lower respiratory tract infections. J. Allergy Clin. Immunol. 155, 436–450.

Zhan, Y., Xu, T., He, F., Guan, W.J., Li, Z., Li, S., Xie, M., Li, X., Chen, R., Cheng, L., Zhong, N., Ye, F., 2021. Clinical evaluation of a metagenomics-based assay for pneumonia management. Front. Microbiol. 12, 751073.

Zhong, H., Wang, Y., Shi, Z., Zhang, L., Ren, H., He, W., Zhang, Z., Zhu, A., Zhao, J., Xiao, F., Yang, F., Liang, T., Ye, F., Zhong, B., Ruan, S., Gan, M., Zhu, J., Li, F., Li, F., Wang, D., Li, J., Ren, P., Zhu, S., Yang, H., Wang, J., Kristiansen, K., Tun, H.M., Chen, W., Zhong, N., Xu, X., Li, Y.M., Li, J., Zhao, J., 2021. Characterization of respiratory microbial dysbiosis in hospitalized COVID-19 patients. Cell Discov 7, 23.